https://ntrs.nasa.gov/search.jsp?R=20030054464 2018-05-15T16:38:38+00:00Z

NASA/TM—2003-212326

Derivation of the Data Reduction Equations for the Calibration of the Six-Component Thrust Stand in the CE–22 Advanced Nozzle Test Facility

Kin C. Wong
Glenn Research Center, Cleveland, Ohio

April 2003

The NASA STI Program Office . . . in Profile

Since its founding, NASA has been dedicated to the advancement of aeronautics and space science. The NASA Scientific and Technical Information (STI) Program Office plays a key part in helping NASA maintain this important role.

The NASA STI Program Office is operated by Langley Research Center, the Lead Center for NASA's scientific and technical information. The NASA STI Program Office provides access to the NASA STI Database, the largest collection of aeronautical and space science STI in the world. The Program Office is also NASA's institutional mechanism for disseminating the results of its research and development activities. These results are published by NASA in the NASA STI Report Series, which includes the following report types:

- TECHNICAL PUBLICATION. Reports of completed research or a major significant phase of research that present the results of NASA programs and include extensive data or theoretical analysis. Includes compilations of significant scientific and technical data and information deemed to be of continuing reference value. NASA's counterpart of peer-reviewed formal professional papers but has less stringent limitations on manuscript length and extent of graphic presentations.

- TECHNICAL MEMORANDUM. Scientific and technical findings that are preliminary or of specialized interest, e.g., quick release reports, working papers, and bibliographies that contain minimal annotation. Does not contain extensive analysis.

- CONTRACTOR REPORT. Scientific and technical findings by NASA-sponsored contractors and grantees.

- CONFERENCE PUBLICATION. Collected papers from scientific and technical conferences, symposia, seminars, or other meetings sponsored or cosponsored by NASA.

- SPECIAL PUBLICATION. Scientific, technical, or historical information from NASA programs, projects, and missions, often concerned with subjects having substantial public interest.

- TECHNICAL TRANSLATION. English-language translations of foreign scientific and technical material pertinent to NASA's mission.

Specialized services that complement the STI Program Office's diverse offerings include creating custom thesauri, building customized databases, organizing and publishing research results . . . even providing videos.

For more information about the NASA STI Program Office, see the following:

- Access the NASA STI Program Home Page at ***http://www.sti.nasa.gov***

- E-mail your question via the Internet to help@sti.nasa.gov

- Fax your question to the NASA Access Help Desk at 301–621–0134

- Telephone the NASA Access Help Desk at 301–621–0390

- Write to:
  NASA Access Help Desk
  NASA Center for AeroSpace Information
  7121 Standard Drive
  Hanover, MD 21076

NASA/TM—2003-212326

Derivation of the Data Reduction Equations for the Calibration of the Six-Component Thrust Stand in the CE–22 Advanced Nozzle Test Facility

Kin C. Wong
Glenn Research Center, Cleveland, Ohio

National Aeronautics and
Space Administration

Glenn Research Center

April 2003

The Propulsion and Power Program at
NASA Glenn Research Center sponsored this work.

Available from

NASA Center for Aerospace Information
7121 Standard Drive
Hanover, MD 21076

National Technical Information Service
5285 Port Royal Road
Springfield, VA 22100

Available electronically at http://gltrs.grc.nasa.gov

Derivation of the Data Reduction Equations for the Calibration of the Six-Component Thrust Stand in the CE–22 Advanced Nozzle Test Facility

Kin C. Wong
National Aeronautics and Space Administration
Glenn Research Center
Cleveland, Ohio 44135

SUMMARY

This paper documents the derivation of the data reduction equations for the calibration of the six-component thrust stand located in the CE–22 Advanced Nozzle Test Facility. The purpose of the calibration is to determine the first-order interactions between the axial, lateral, and vertical load cells (second-order interactions are assumed to be negligible).

In an ideal system, the measurements made by the thrust stand along the three coordinate axes should be independent. For example, when a test article applies an axial force on the thrust stand, the axial load cells should measure the full magnitude of the force, while the off-axis load cells (lateral and vertical) should read zero. Likewise, if a lateral force is applied, the lateral load cells should measure the entire force, while the axial and vertical load cells should read zero. However, in real-world systems, there may be interactions between the load cells. Through proper design of the thrust stand, these interactions can be minimized, but are hard to eliminate entirely. Therefore, the purpose of the thrust stand calibration is to account for these interactions, so that necessary corrections can be made during testing. These corrections can be expressed in the form of an interaction matrix, and this paper shows the derivation of the equations used to obtain the coefficients in this matrix.

SYMBOLS

$CX1$	Aft-left axial calibration load cell
$CX2$	Aft-right axial calibration load cell
$CY1$	Forward-right lateral calibration load cell
$CY2$	Aft-right lateral calibration load cell
$CZ1$	Forward-left vertical calibration load cell
$CZ2$	Forward-right vertical calibration load cell
$CZ3$	Aft-left vertical calibration load cell
$CZ4$	Aft-right vertical calibration load cell
$RX1$	Aft-left axial reaction load cell
$RX2$	Aft-right axial reaction load cell
$RY1$	Forward-left lateral reaction load cell
$RY2$	Aft-left lateral reaction load cell
$RZ1$	Forward-left vertical reaction load cell

$RZ2$	Forward-right vertical reaction load cell
$RZ3$	Aft-left vertical reaction load cell
$RZ4$	Aft-right vertical reaction load cell
FX	Axial force, or force in the x-direction
FY	Lateral force, or force in the y-direction
FZ	Vertical force, or force in the z-direction
MX	Rolling moment, or moment about the x-axis
MY	Pitching moment, or moment about the y-axis
MZ	Yawing moment, or moment about the z-axis
$[F_{MX}]$	The 5×1 force matrix that contains the rolling moment component
$[F_{MY}]$	The 5×1 force matrix that contains the pitching moment component
$[R]$	The 5×1 reaction load cell matrix that contains the rolling moment component
$[Q]$	The 5×1 reaction load cell matrix that contains the pitching moment component
$[S]$	The 5×5 interaction matrix that contains the coefficients for the rolling moment calculation
$[U]$	The 5×5 interaction matrix that contains the coefficients for the pitching moment calculation
s_{ij}	The coefficients in the matrix $[S]$
u_{ij}	The coefficients in the matrix $[U]$
σ_{ij}	The coefficients in the matrix $[S]^{-1}$
μ_{ij}	The coefficients in the matrix $[U]^{-1}$
L_{P_1}	Forward moment arm for the pitching moment (distance from centroid to the $CZ1$ and $CZ2$ load cells)
L_{P_2}	Aft moment arm for the pitching moment (distance from centroid to the $CZ3$ and $CZ4$ load cells)
L_Y	Moment arm for the yawing moment (distance from centroid to the $CY1$ and $CY2$ load cells)
L_R	Moment arm for the rolling moment (distance from centroid to the $CZ1$ and $CZ3$ load cells, and to the $CZ2$ and $CZ4$ load cells)

THE CE–22 NOZZLE TEST FACILITY

The CE–22 Advanced Nozzle Test Facility is located in the Engine Research Building (ERB) at the NASA Glenn Research Center. A schematic of the CE–22 Test Facility is shown in figure 1. The test section consists of a 23-ft long by 7-½-foot-inside-diameter vacuum tank. The upstream section is fixed while the downstream section slides open on rails, allowing for easy access to the test model. An inflatable rubber seal is used to prevent leakage when the two halves are closed for testing.

The inlet air and exhaust is supplied by compressors and exhausters operated by Central Process Systems (CPS). The primary air system can supply inlet air at a pressure of 40 psig with a maximum flow rate of 40 lbm/sec. There are also provisions for two one-inch secondary supply lines that enter through the top of the test tank. The secondary air

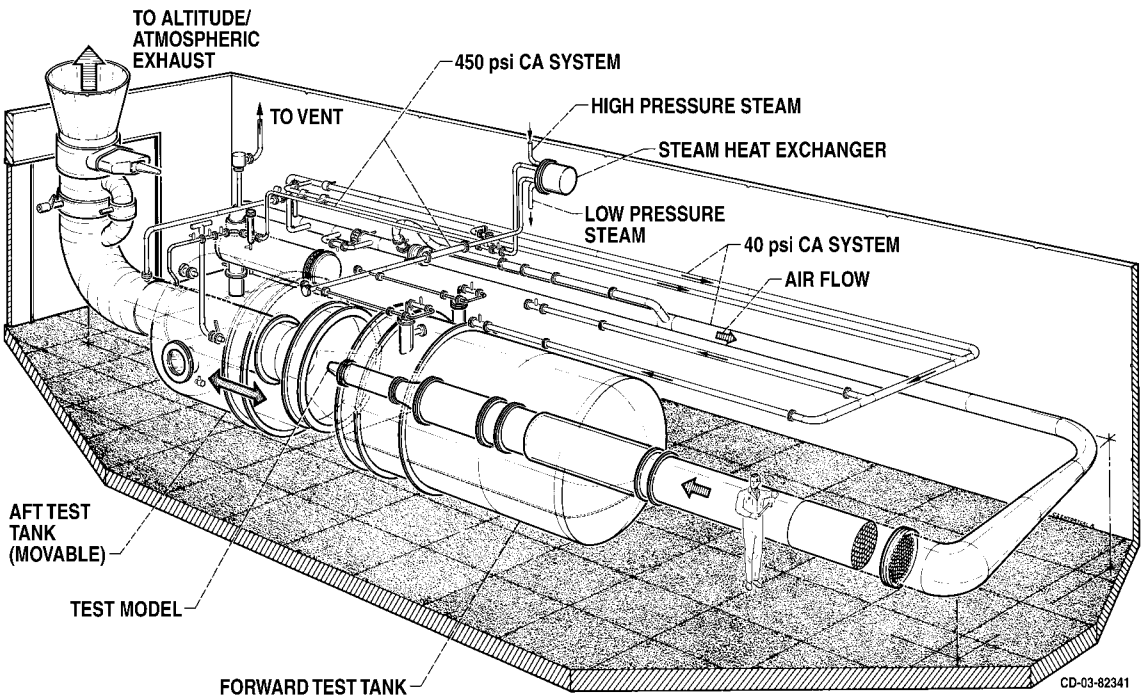

Figure 1.—The NASA Glenn Research Center Nozzle Test Facility (CE-22).

can be supplied at 40, 150, or 450 psig with maximum flow rates of 21, 2, and 10 lbm/sec, respectively. The exhaust system can pull a vacuum down to approximately 1.9 psia to simulate altitude conditions at 48,000 feet.

The CE–22 Test Facility also has a six-component thrust stand, which allows for simultaneous force and moment measurements along the three coordinate axes. The thrust stand and the altitude capability make the CE–22 Test Facility a unique asset to NASA. The facility is ideally suited for testing sub-scale advanced aircraft nozzle concepts which employ thrust vectoring. For further details about the CE–22 Test Facility, refer to references (1) and (2).

THE SIX-COMPONENT THRUST STAND

The installation of the thrust stand is shown in figure 2. The thrust stand is comprised of two major parts: the ground frame and the live frame. The ground frame is bolted to the floor of the test tank and the live frame is in turn attached to the ground frame through the 8 reaction load cells. The inlet piping and the experimental model are mounted to the live frame. Thus, forces produced by the experimental model cause a displacement of the live frame relative to the ground frame. This displacement, on the order of thousandths of an inch, is converted to a voltage by each of the 8 reaction load cells. This voltage is then converted to a force reading by the data acquisition system. The interaction matrix is then applied by the data acquisition program to correct the individual force readings to take into account the interactions between the load cells.

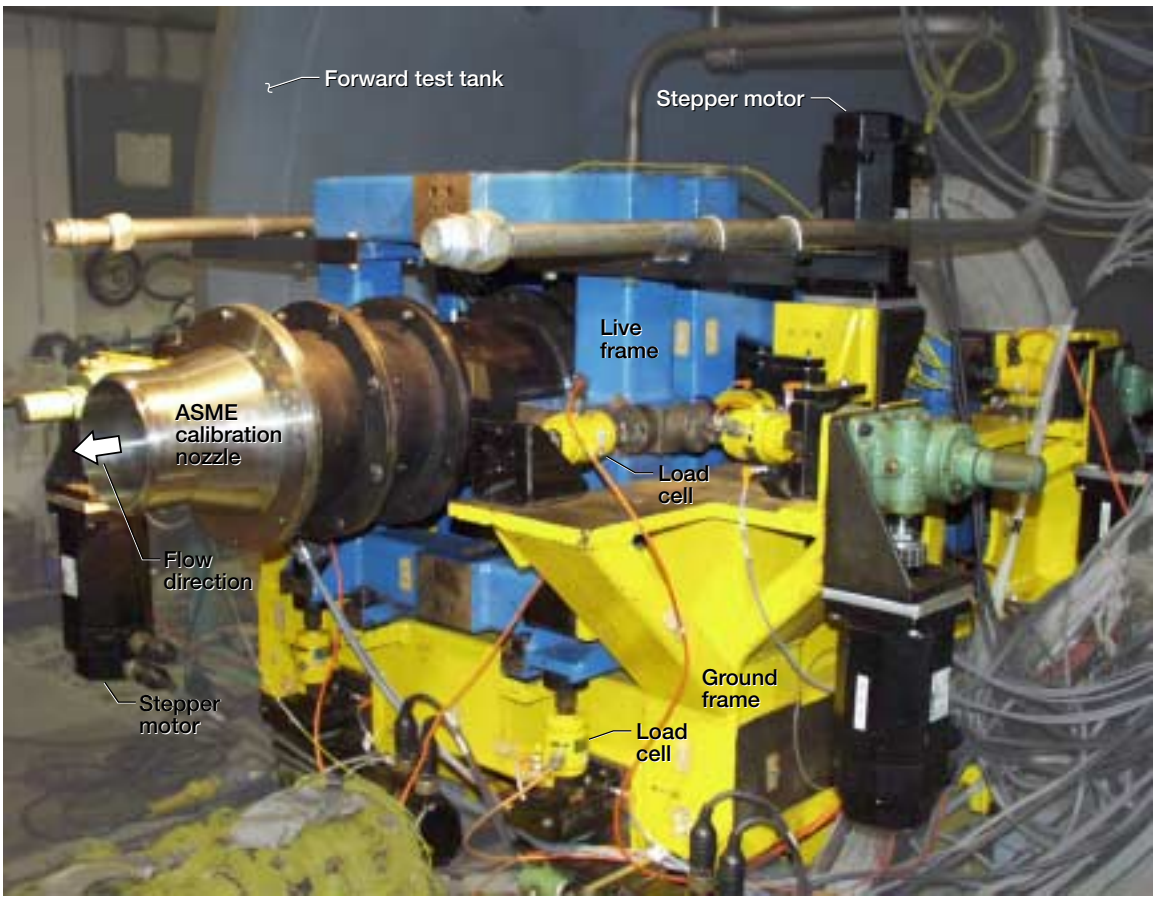

Figure 2.—The six component thrust stand.

There are three other items concerning the operation of the thrust stand that need mentioning: (1) There is a metric break that is located in the inlet air supply line just upstream of the thrust stand. The metric break is a physical break in the piping that isolates the experimental model and the part of the piping attached to the live frame of the thrust stand from the rest of the upstream air supply line. This break in the air supply line is enclosed by a labyrinth seal to minimize leakage; (2) The live frame of the thrust stand is actually comprised of two parts joined together by an elastic hinge. The purpose of this elastic hinge is to minimize the interaction between the axial and the lateral components. Because of the elastic hinge, off-center axial forces will not produce a yawing moment. A yawing moment can only be produced by offset lateral forces; and (3) the weight of the live frame, the piping, and the experimental model are zeroed out before the start of each test run.

Figure 3 shows a schematic of the thrust stand. The sign convention used is as follows. The axial direction, or x-axis, is positive in the upstream direction. The lateral direction, or y-axis, is positive on the right hand side, aft-looking-forward. And the vertical direction, or z-axis, is positive in the downward direction. The terms used for the forces and moments are summarized in Table I.

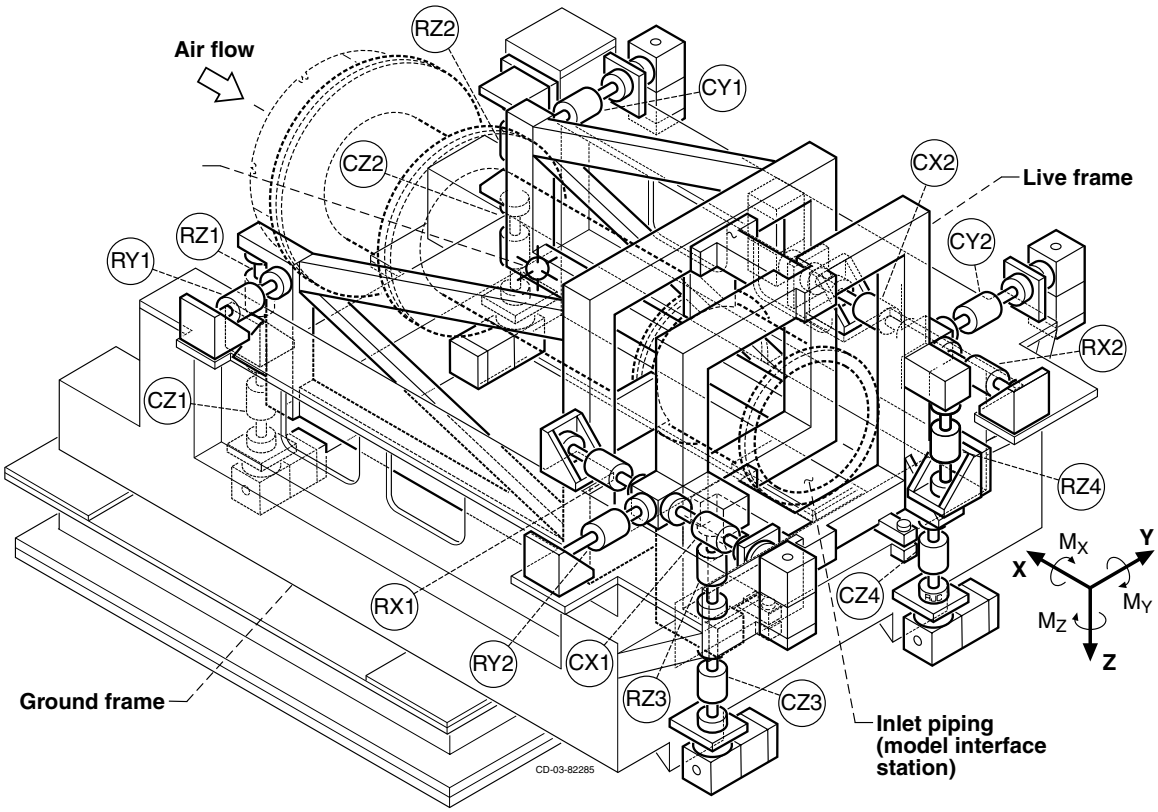

Figure 3.—Schematic of the thrust stand showing location of load cells.

Table I: Symbols and Terms Used for Forces and Moments.

Symbol	Force or Moment
FX	Axial force, or force in the x-direction
FY	Lateral force, or force in the y-direction
FZ	Vertical force, or force in the z-direction
MX	Rolling moment, or moment about the x-axis
MY	Pitching moment, or moment about the y-axis
MZ	Yawing moment, or moment about the z-axis

LOAD CELL DESCRIPTION

As previously mentioned, there are 8 reaction load cells that measure forces by detecting the displacement of the live frame relative to the ground frame. In addition, there are 8 calibration load cells mounted in-line with the 8 reaction load cells. These calibration load cells are used to measure the applied load on the thrust stand during calibration.

The calibration load cells are designated by a C (e.g., *CX*1, *CY*1, etc.) and the reaction load cells with an R (e.g., *RX*1, *RY*1, etc). The positions of the 8 reaction load cells are summarized in Table II, and their exact locations relative to the centroid are shown in

Table II: Load Cell Locations.

Load Cell	Location
$RX1$	Aft-Left
$RX2$	Aft-Right
$RY1$	Forward-Left
$RY2$	Aft-Left
$RZ1$	Forward-Left
$RZ2$	Forward-Right
$RZ3$	Aft-Left
$RZ4$	Aft-Right

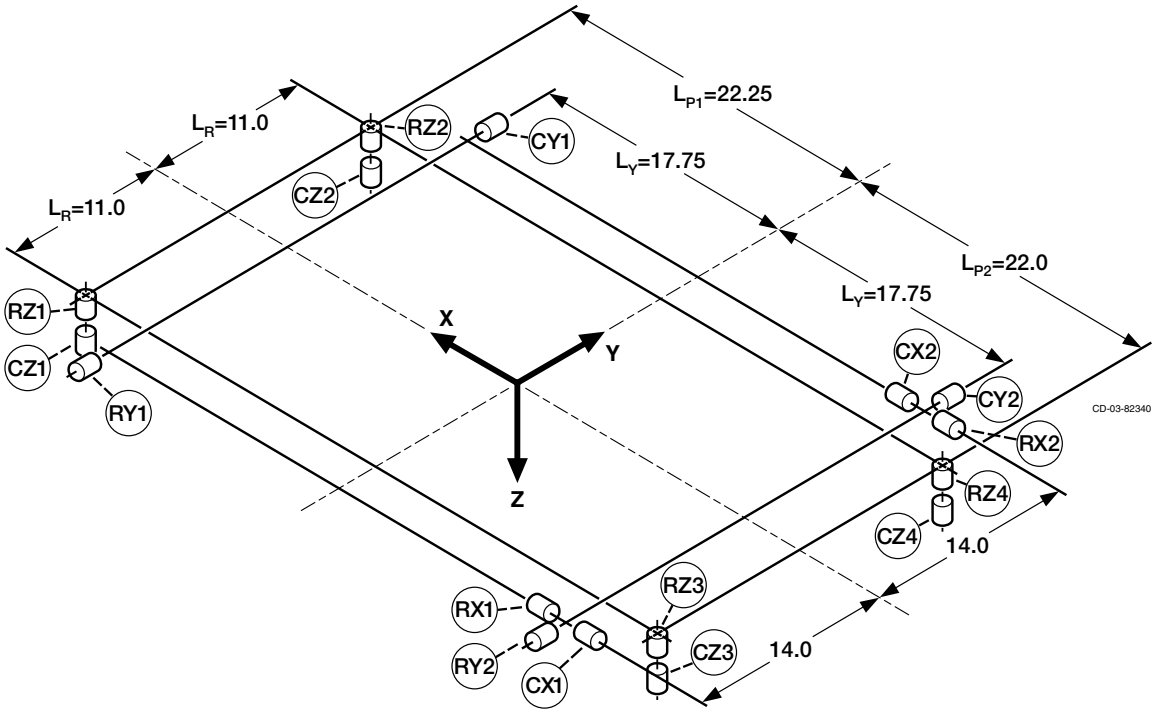

Figure 4. —Schematic of Load Cell locations.

figure 4. Forward and aft is relative to the direction of the airflow, and left and right is referenced from an aft-looking-forward perspective.

Before the thrust stand itself is calibrated, each of the 16 load cells (8 calibration and 8 reaction load cells) are sent out for calibration at the calibration laboratory. The load cells are calibrated against a standard that can be traced to a national standard. Each individual load cell works by converting a displacement into an electrical voltage. The calibration laboratory applies a known force on the load cell and plots a Force versus Voltage curve. This curve should be linear within the working range of the load cell. Once the slope and intercept from this plot are determined, these constants are entered into the data acquisition program. During an experiment, the displacement of the thrust stand is

measured as a voltage from the load cells, which in turn is converted to a force by the data acquisition system.

A close-up of one of the vertical load cell pairs mounted on the thrust stand is shown in figure 5. The metal fixtures on each end of the load cell are flexures. Their job is to minimize the effect of off-axis forces on the load cell. Thus, ideally, an axial force produced by the experimental model is measured only through the axial load cells and should have little or no affect on the lateral and vertical load cells.

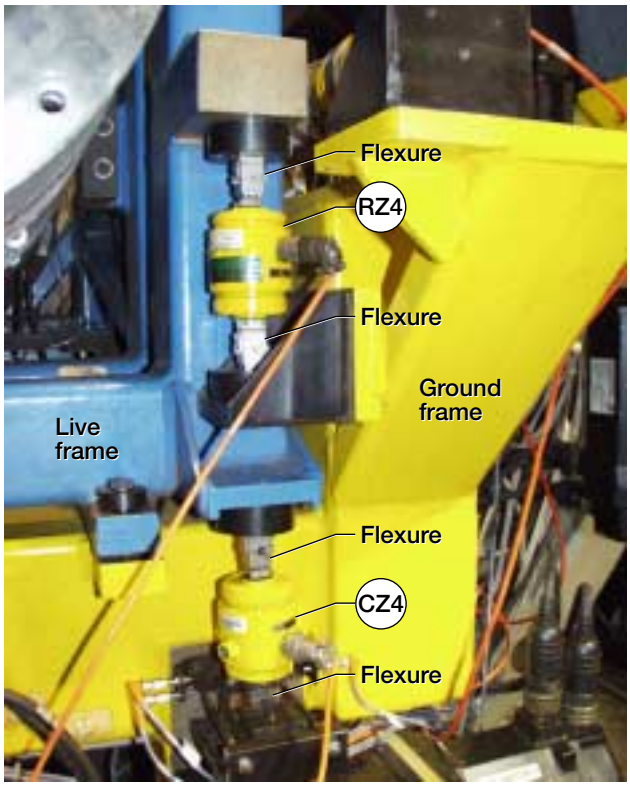

Figure 5.—Calibration/reaction load cell pair.

CALIBRATION PROCEDURE

The purpose of the thrust stand calibration is to determine the first-order interactions between the load cells. For example, what effect does applying an axial force have on the vertical load cells? When a 100 lb. force in the x-direction is applied, one would expect the sum of the axial load cells to read 100 lbs. But due to constraints from the other attached load cells, this force may not be exactly 100 lbs. In addition, a force may be induced on the lateral and or vertical load cells. If the thrust stand is designed properly, such interactions can be minimized, but are hard to eliminate completely. The purpose of the calibration is to obtain a correction factor to account for these interactions. This correction factor is expressed as a matrix and is referred to interchangeably as the interaction matrix or the calibration matrix.

The calibration of the thrust stand is performed by applying known forces and moments and recording its effects on the reaction load cells. Forces are applied through the use of the stepper motors mounted in-line with the calibration load cells. The calibration load cells are used to determine the amount of force applied by the stepper motor. Forces and moments are applied in the manner shown in Table III. The first column indicates the type of load applied to the thrust stand. The second column indicates the calibration load cells used to measure this applied load. For the applied moments, the load is applied on one side of the thrust stand, then on the other side, as indicated by the "/". The third column shows the range and increment of the applied loads. The range and increment may be adjusted depending on the range of interest for upcoming test programs.

As an example, when applying the moment about the y-axis, or *MY*, the stepper motors in line with *CZ*1 and *CZ*2 are activated to apply 0, –25, –50, –75, –100, –125, –100, –75, –50, –25, and 0 lbs. each to the thrust stand. The load is then applied in the other direction from 0 to 100 lbs. and back down to 0. At each point the readings indicated by the 8 reaction load cells are recorded. Readings are taken on the way up and on the way back down to determine the repeatability of the thrust stand. The same procedure is then repeated for the stepper motors mounted in-line with *CZ*3 and *CZ*4.

Table III: Calibration Loadings.

Applied Force or Moment	Calibration Load Cell(s) used to Measure Applied Load	Range and Increment of Applied Load
FZ	*CX*1, *CX*2	0 to 3000, in. 250 lb increments
FY	*CY*1, *CY*2	0 to –500 and 0 to 500, in 100 lb increments
FZ	*CZ*1, *CZ*2, *CZ*3, *CZ*4	0 to –250 and 0 to 250, in 50 lb increments
MX	*CZ*1, *CZ*3 / *CZ*2, *CZ*4	0 to –250 and 0 to 250, in 50 lb increments
MY	*CZ*1, *CZ*2 / *CZ*3, *CZ*4	0 to –250 and 0 to 250, in 50 lb increments
MZ	*CY*1 / *CY*2	0 to –500 and 0 to 500, in 100 lb increments

The applied calibration loads are split equally between the two load cells when the *FX*, *FY*, *MY*, and *MZ* loads are applied. However, when the *CZ*1 and *CZ*3 (or *CZ*2 and *CZ*4) load cells are loaded together, as in the case when applying the *FZ* and *MX* loads, care must be taken in order to prevent an unwanted pitching moment. Due to the fact that the forward vertical load cells (*CX*1 and *CX*2) have a different moment arm than the aft vertical load cells (*CX*3 and *CX*4), the forces must be applied such that:

$$CZ1 = CZ2\,, \tag{1}$$

$$CZ3 = CZ4\,, \tag{2}$$

and

$$CZ1 = \frac{L_{p_2}}{L_{p_1}} \cdot CZ3\,, \tag{3}$$

where L_{P_1} = 22.25 in. is the distance along the x-axis from the centroid to *CZ*1 and *CX*2, and L_{P_2} = 22.0 in. is the distance along the x-axis from the centroid to *CZ*3 and *CZ*4.

THE FORCE AND MOMENT EQUATIONS

The basic equation used to calculate forces and moments is:

$$[F] = [S][R], \tag{4}$$

where $[F]$ is a 6×1 matrix containing the 3 forces and 3 moments to be measured, [*R*] is the 8×1 matrix containing the 8 reaction load cell readings, and [*S*] is the interaction or calibration matrix. During the calibration, known forces and moments, [*F*], are applied to the thrust stand and the load cell readings, [*R*], are recorded from the data system. In order to obtain [*S*], its inverse, $[S]^{-1}$, must be determined from the following form of equation (4):

$$[S]^{-1}[F] = [R] \tag{5}$$

The problem with modeling the system using equations (4) and (5) is that [*S*] is a 6×8 matrix, and is therefore not invertible. In other words, because there are 8 reaction load cells and only 6 components that need to be resolved, the system is indeterminate. The way around this problem is to divide the system into two parts. (This technique was developed by Roger Werner, 1991, NASA Glenn Research Center, OH, personal communication.) The load cells are combined, as shown below, so that there are 5 load cell readings and 5 components in each system. The two systems are represented below as:

$$[F_{MX}] = [S][R] \tag{6}$$

$$\begin{bmatrix} FX \\ FY \\ FZ \\ MX \\ MZ \end{bmatrix} = \begin{bmatrix} s_{11} & s_{12} & s_{13} & s_{14} & s_{15} \\ s_{21} & s_{22} & s_{23} & s_{24} & s_{25} \\ s_{31} & s_{32} & s_{33} & s_{34} & s_{35} \\ s_{41} & s_{42} & s_{43} & s_{44} & s_{45} \\ s_{51} & s_{52} & s_{53} & s_{54} & s_{55} \end{bmatrix} \begin{bmatrix} RX1 + RX2 \\ RY1 \\ RY2 \\ RZ1 + RZ3 \\ RZ2 + RZ4 \end{bmatrix} \tag{7}$$

$$\left[F_{MY}\right] = [U][Q] \tag{8}$$

$$\begin{bmatrix} FX \\ FY \\ FZ \\ MY \\ MZ \end{bmatrix} = \begin{bmatrix} u_{11} & u_{12} & u_{13} & u_{14} & u_{15} \\ u_{21} & u_{22} & u_{23} & u_{24} & u_{25} \\ u_{31} & u_{32} & u_{33} & u_{34} & u_{35} \\ u_{41} & u_{42} & u_{43} & u_{44} & u_{45} \\ u_{51} & u_{52} & u_{53} & u_{54} & u_{55} \end{bmatrix} \begin{bmatrix} RX1 + RX2 \\ RY1 \\ RY2 \\ RZ1 + RZ2 \\ RZ3 + RZ4 \end{bmatrix} \tag{9}$$

In equation (7), the vertical load cells are combined left ($RZ1 + RZ3$) and right ($RZ2 + RZ4$) such that they produce a rolling moment, while in equation (9), the vertical load cells are combined forward ($RZ1 + RZ2$) and aft ($RZ3 + RZ4$) such that they produce a pitching moment. See figure 3 for the load cell locations.

In addition, the $RX1$ and $RX2$ terms are combined, while the $RY1$ and $RY2$ terms are kept separate. This is due to the elastic hinge. Because of this elastic hinge, an offset axial force would not produce a yawing moment; therefore, the terms can be combined. The $RY1$ and $RY2$ terms need to remain separate in order to resolve the yawing moment, MZ.

Both $[F_{MX}]$ and $[F_{MY}]$ are usually calculated by the data acquisition program during an experiment. But because nozzles usually provide pitch and/or yaw vectoring, the components in $[F_{MY}]$ are more relevant since it contains the equation for the pitching moment. The calculation of $[F_{MX}]$ serves as a check on $[F_{MY}]$, and is also used to monitor the test article for unexpected rolling moments.

THE INTERACTION MATRICES

In order to better illustrate the function of the interaction matrix, the FX component as represented in equation (7) is written out as follows:

$$FX = s_{11}(RX1 + RX2) + s_{12}RY1 + s_{13}RY2 + s_{14}(RZ1 + RZ3) + s_{15}(RZ2 + RZ4) \tag{10}$$

In this form, it is easier to see what each of the coefficients represents. For instance, the coefficient s_{11} represents the weighting factor for the effect of the sum of the two axial load cells, $RX1$ and $RX2$, on FX. The coefficient s_{12} represents the weighting factor for the effect of the $RY1$ load cell on FX, and so on. Thus, for small interactions, one would expect the coefficient s_{11} to be approximately one, and the other coefficients (s_{12}, s_{13}, s_{14}, and s_{15}) to be close to zero.

To get a better feel for the expected values of the coefficients in the interaction matrices $[S]$ and $[U]$, assume for the moment that there are no interactions between the load cells. If this were the case, it is expected that the axial force would be the sum of the two axial load cells ($RX1 + RX2$), the lateral force would be the sum of the two lateral load cells ($RY1 + RY2$), and the vertical force would be the sum of the four vertical load cells

($RZ1 + RZ2 + RZ3 + RZ4$). Similarly, the moments would be equal to the product of the applied force and its corresponding moment arm (see figure 4 for the lengths of the moment arms). For this ideal case, the following equations would be used to determine the three forces and three moments:

$$FX = RX1 + RX2 \tag{11}$$

$$FY = RY1 + RY2 \tag{12}$$

$$FZ = RZ1 + RZ2 + RZ3 + RZ4 \tag{13}$$

$$MX = L_R \times (RZ1 + RZ3) + L_R \times (RZ2 + RZ4) \tag{14}$$

$$MY = L_{P_1} \times (RZ1 + RZ2) + L_{P_2} \times (RZ3 + RZ4) \tag{15}$$

$$MZ = L_Y \times RY1 + L_Y \times RY2 \tag{16}$$

These equations can be represented in the form of equations (7) and (9) as:

$$\begin{bmatrix} FX \\ FY \\ FZ \\ MX \\ MZ \end{bmatrix} = \begin{bmatrix} 1 & 0 & 0 & 0 & 0 \\ 0 & 1 & 1 & 0 & 0 \\ 0 & 0 & 0 & 1 & 1 \\ 0 & 0 & 0 & L_R & L_R \\ 0 & L_Y & L_Y & 0 & 0 \end{bmatrix} \begin{bmatrix} RX1 + RX2 \\ RY1 \\ RY2 \\ RZ1 + RZ3 \\ RZ2 + RZ4 \end{bmatrix} \tag{17}$$

$$\begin{bmatrix} FX \\ FY \\ FZ \\ MY \\ MZ \end{bmatrix} = \begin{bmatrix} 1 & 0 & 0 & 0 & 0 \\ 0 & 1 & 1 & 0 & 0 \\ 0 & 0 & 0 & 1 & 1 \\ 0 & 0 & 0 & L_{P_1} & L_{P_2} \\ 0 & L_Y & L_Y & 0 & 0 \end{bmatrix} \begin{bmatrix} RX1 + RX2 \\ RY1 \\ RY2 \\ RZ1 + RZ2 \\ RZ3 + RZ4 \end{bmatrix} \tag{18}$$

Again, equations (17) and (18) represent the ideal case where there are no interactions between the load cells. However, for small interactions, the coefficients for the [*S*] and [*U*] matrices obtained from the calibration should be fairly close to the above values. Thus the values in equations (17) and (18) can be used as a sanity check to determine if the calibration and data reduction were done correctly.

DERIVATION OF THE INTERACTION MATRIX COEFFICIENTS

The previous sections explained how the interaction matrices, [*S*] and [*U*], are used to correct the forces and moments measured by the thrust stand. The following sections will explain the method by which the coefficient terms in the interaction matrices are derived.

Equations (7) and (9), rewritten in the form of equation (5), are shown below:

$$[S]^{-1}[F_{MX}] = [R] \tag{19}$$

$$\begin{bmatrix} \sigma_{11} & \sigma_{12} & \sigma_{13} & \sigma_{14} & \sigma_{15} \\ \sigma_{21} & \sigma_{22} & \sigma_{23} & \sigma_{24} & \sigma_{25} \\ \sigma_{31} & \sigma_{32} & \sigma_{33} & \sigma_{34} & \sigma_{35} \\ \sigma_{41} & \sigma_{42} & \sigma_{43} & \sigma_{44} & \sigma_{45} \\ \sigma_{51} & \sigma_{52} & \sigma_{53} & \sigma_{54} & \sigma_{55} \end{bmatrix} \begin{bmatrix} FX \\ FY \\ FZ \\ MX \\ MZ \end{bmatrix} = \begin{bmatrix} RX1 + RX2 \\ RY1 \\ RY2 \\ RZ1 + RZ3 \\ RZ2 + RZ4 \end{bmatrix} \tag{20}$$

$$[U]^{-1}[F_{MY}] = [Q] \tag{21}$$

$$\begin{bmatrix} \mu_{11} & \mu_{12} & \mu_{13} & \mu_{14} & \mu_{15} \\ \mu_{21} & \mu_{22} & \mu_{23} & \mu_{24} & \mu_{25} \\ \mu_{31} & \mu_{32} & \mu_{33} & \mu_{34} & \mu_{35} \\ \mu_{41} & \mu_{42} & \mu_{43} & \mu_{44} & \mu_{45} \\ \mu_{51} & \mu_{52} & \mu_{53} & \mu_{54} & \mu_{55} \end{bmatrix} \begin{bmatrix} FX \\ FY \\ FZ \\ MY \\ MZ \end{bmatrix} = \begin{bmatrix} RX1 + RX2 \\ RY1 \\ RY2 \\ RZ1 + RZ2 \\ RZ3 + RZ4 \end{bmatrix} \tag{22}$$

Equations (20) and (22) are the basis for the calibration data reduction equations. The idea here is to apply a single known force or moment, for example, *FX*, record the reaction load cell readings, *RX*1 + *RX*2, *RY*1, etc., and determine the individual coefficients σ and μ. Once the individual coefficients are determined, the $[S]^{-1}$ and $[U]^{-1}$ matrices are inverted to obtain the interaction matrices [*S*] and [*U*]. The next three sections explain in detail how this is done. Examples are given for the axial force (*FX*), the pitching moment (*MY*), and the yawing moment (*MZ*) calibrations.[1] The lateral force (*FY*) and vertical force (*FZ*) calibrations are similar to the axial force calibration, and the rolling moment (*MX*) calibration is similar to the pitching moment calibration.

[1] The term axial force calibration is used to indicate the loading of the axial calibration force. The axial force is not "calibrated" until all the interaction coefficients are determined from all the different loadings. Likewise for the terms lateral force calibration, pitching moment calibration, etc.

THE EQUATIONS FOR THE *FX* CALIBRATION

For the axial force calibration, the stepper motors in line with the $CX1$ and $CX2$ load cells are used to apply the loads shown previously in Table III. For this case, all the terms in $[F_{MX}]$ are zero except for FX. Thus, equation (20) becomes:

$$\begin{bmatrix} \sigma_{11} & \sigma_{12} & \sigma_{13} & \sigma_{14} & \sigma_{15} \\ \sigma_{21} & \sigma_{22} & \sigma_{23} & \sigma_{24} & \sigma_{25} \\ \sigma_{31} & \sigma_{32} & \sigma_{33} & \sigma_{34} & \sigma_{35} \\ \sigma_{41} & \sigma_{42} & \sigma_{43} & \sigma_{44} & \sigma_{45} \\ \sigma_{51} & \sigma_{52} & \sigma_{53} & \sigma_{54} & \sigma_{55} \end{bmatrix} \begin{bmatrix} FX \\ 0 \\ 0 \\ 0 \\ 0 \end{bmatrix} = \begin{bmatrix} RX1 + RX2 \\ RY1 \\ RY2 \\ RZ1 + RZ3 \\ RZ2 + RZ4 \end{bmatrix} \tag{23}$$

From this, the first column of the inverse matrix can be determined. Writing out the individual equations in the system, discarding the zero terms, and solving for σ_{i1}, equation (23) becomes:

$$\sigma_{11} FX = RX1 + RX2 \quad \Rightarrow \quad \sigma_{11} = \frac{RX1 + RX2}{FX} \tag{24}$$

$$\sigma_{21} FX = RY1 \quad \Rightarrow \quad \sigma_{21} = \frac{RY1}{FX} \tag{25}$$

$$\sigma_{31} FX = RY2 \quad \Rightarrow \quad \sigma_{31} = \frac{RY2}{FX} \tag{26}$$

$$\sigma_{41} FX = RZ1 + RZ3 \quad \Rightarrow \quad \sigma_{41} = \frac{RZ1 + RZ3}{FX} \tag{27}$$

$$\sigma_{51} FX = RZ2 + RZ4 \quad \Rightarrow \quad \sigma_{51} = \frac{RZ2 + RZ4}{FX} \tag{28}$$

Each of the σ_{i1} terms can be determined from the slope of the plot of the corresponding load cell readings versus FX. For example, the coefficient σ_{11} is the value of the slope of the plot of $RX1 + RX2$ versus FX.

The coefficients μ_{i1}, for the matrix $[U]^{-1}$ are found in a the same manner:

$$\mu_{11} = \frac{RX1 + RX2}{FX} \tag{29}$$

$$\mu_{21} = \frac{RY1}{FX} \tag{30}$$

$$\mu_{31} = \frac{RY2}{FX} \tag{31}$$

$$\mu_{41} = \frac{RZ1 + RZ2}{FX} \tag{32}$$

$$\mu_{51} = \frac{RZ3 + RZ4}{FX} \tag{33}$$

Similarly, the *FY* and *FZ* calibrations will produce the coefficients σ_{i2} and σ_{i3} for $[S]^{-1}$, and the coefficients μ_{i2} and μ_{i3} for $[U]^{-1}$.

THE EQUATIONS FOR THE *MY* CALIBRATION

The coefficients for the moment calibrations are determined in a similar fashion as the pure force calibrations, except there is an extra term due to the fact that an offset vertical force is used to produce the moment. For the *MY* calibration, the pitching moments are applied through two separate loadings. Forces are first applied through the stepper motors in line with the forward vertical load cells, *CZ*1 and *CZ*2. The procedure is then repeated with the aft vertical load cells, *CZ*3 and *CZ*4. The coefficients are computed separately for each loading, and then averaged in the final result. For both cases, the non-zero components of $[F_{MY}]$ are *FZ* and *MY*. Therefore, equation (22) becomes:

$$\begin{bmatrix} \mu_{11} & \mu_{12} & \mu_{13} & \mu_{14} & \mu_{15} \\ \mu_{21} & \mu_{22} & \mu_{23} & \mu_{24} & \mu_{25} \\ \mu_{31} & \mu_{32} & \mu_{33} & \mu_{34} & \mu_{35} \\ \mu_{41} & \mu_{42} & \mu_{43} & \mu_{44} & \mu_{45} \\ \mu_{51} & \mu_{52} & \mu_{53} & \mu_{54} & \mu_{55} \end{bmatrix} \begin{bmatrix} 0 \\ 0 \\ FZ \\ MY \\ 0 \end{bmatrix} = \begin{bmatrix} RX1 + RX2 \\ RY1 \\ RY2 \\ RZ1 + RZ2 \\ RZ3 + RZ4 \end{bmatrix} \tag{34}$$

Writing out each of the individual equations, discarding the zero terms, and solving for μ_{i4}, equation (34) becomes:

$$\mu_{13}FZ + \mu_{14}L_pFZ = RX1 + RX2 \quad \Rightarrow$$

$$\mu_{14} = \frac{1}{L_P}\left(\frac{RX1 + RX2}{FZ} - \mu_{13}\right) \tag{35}$$

$$\mu_{23}FZ + \mu_{24}L_pFZ = RY1 \quad \Rightarrow$$

$$\mu_{24} = \frac{1}{L_P}\left(\frac{RY1}{FZ} - \mu_{23}\right) \tag{36}$$

$$\mu_{33}FZ + \mu_{34}L_pFZ = RY2 \quad \Rightarrow$$

$$\mu_{34} = \frac{1}{L_P}\left(\frac{RY2}{FZ} - \mu_{33}\right) \tag{37}$$

$$\mu_{43}FZ + \mu_{44}L_pFZ = RZ1 + RZ2 \qquad \Rightarrow$$

$$\mu_{44} = \frac{1}{L_P}\left(\frac{RZ1 + RZ2}{FZ} - \mu_{43}\right) \tag{38}$$

$$\mu_{53}FZ + \mu_{54}L_pFZ = RZ3 + RZ4 \qquad \Rightarrow$$

$$\mu_{54} = \frac{1}{L_P}\left(\frac{RZ3 + RZ4}{FZ} - \mu_{53}\right) \tag{39}$$

The μ_{i3} terms in the above equations are determined from the *FZ* calibration and the ratios ($\frac{RX1 + RX2}{FZ}$, $\frac{RY1}{FZ}$, etc.) are determined from the slope of the plot of the corresponding load cell readings versus the applied force, *FZ*.

The σ_{i4} terms are determined in a similar fashion through the *MX* calibration.

THE EQUATIONS FOR THE *MZ* CALIBRATION

For the *MZ* calibration, the yawing moments are applied through two separate loadings. Forces are first applied through the stepper motor in line with the *CY*1 load cell. The procedure is then repeated for the *CY*2 load cell. The coefficients are computed separately for each loading, and then averaged in the final result. In this case, equation (20) becomes:

$$\begin{bmatrix} \sigma_{11} & \sigma_{12} & \sigma_{13} & \sigma_{14} & \sigma_{15} \\ \sigma_{21} & \sigma_{22} & \sigma_{23} & \sigma_{24} & \sigma_{25} \\ \sigma_{31} & \sigma_{32} & \sigma_{33} & \sigma_{34} & \sigma_{35} \\ \sigma_{41} & \sigma_{42} & \sigma_{43} & \sigma_{44} & \sigma_{45} \\ \sigma_{51} & \sigma_{52} & \sigma_{53} & \sigma_{54} & \sigma_{55} \end{bmatrix} \begin{bmatrix} 0 \\ FY \\ 0 \\ 0 \\ MZ \end{bmatrix} = \begin{bmatrix} RX1 + RX2 \\ RY1 \\ RY2 \\ RZ1 + RZ3 \\ RZ2 + RZ4 \end{bmatrix} \tag{40}$$

Writing out each of the individual equations, discarding the zero terms, and solving for σ_{i5}, equation (40) becomes:

$$\sigma_{12}FY + \sigma_{15}L_YFY = RX1 + RX2 \qquad \Rightarrow$$

$$\sigma_{15} = \frac{1}{L_Y}\left(\frac{RX1 + RX2}{FY} - \sigma_{12}\right) \tag{41}$$

$$\sigma_{22}FY + \sigma_{25}L_YFY = RY1 \qquad \Rightarrow$$

$$\sigma_{25} = \frac{1}{L_Y}\left(\frac{RY1}{FY} - \sigma_{22}\right) \tag{42}$$

$$\sigma_{32}FY + \sigma_{35}L_YFY = RY2 \qquad \Rightarrow$$

$$\sigma_{35} = \frac{1}{L_Y}\left(\frac{RY2}{FY} - \sigma_{32}\right) \tag{43}$$

$$\sigma_{42}FY + \sigma_{45}L_Y FY = RZ1 + RZ3 \quad \Rightarrow$$

$$\sigma_{45} = \frac{1}{L_Y}\left(\frac{RZ1 + RZ3}{FY} - \sigma_{42}\right) \tag{44}$$

$$\sigma_{52}FY + \sigma_{55}L_Y FY = RZ2 + RZ4 \quad \Rightarrow$$

$$\sigma_{55} = \frac{1}{L_Y}\left(\frac{RZ2 + RZ4}{FY} - \sigma_{52}\right) \tag{45}$$

The σ_{i2} terms in the above equations are determined from the FY calibration and the ratios ($\frac{RX1 + RX2}{FY}$, $\frac{RY1}{FY}$, etc.) are determined from the slope of the plot of the corresponding load cell readings verus the applied force, FY.

The μ_{i5} terms for the $[U]^{-1}$ matrix are found in a similar fashion.

SUMMARY OF THE INTERACTION COEFFICIENTS

A summary of all the equations used for determining the coefficients in the $[S]^{-1}$ and $[U]^{-1}$ matrices are shown in Tables IV and V. Once all the coefficients for the inverse matrices are found, the matrices can be inverted to obtain the interaction matrices $[S]$ and $[U]$. A sample set of calibration data is listed in Appendix A.

Table IV: Coefficients σ_{ij} for the $[S]^{-1}$ Matrix

$i \backslash j$	1	2	3	4	5
1	$\frac{\Delta(RX1+RX2)}{\Delta FX}$	$\frac{\Delta(RX1+RX2)}{\Delta FY}$	$\frac{\Delta(RX1+RX2)}{\Delta FZ}$	$\frac{1}{L_R}\left(\frac{\Delta(RX1+RX2)}{\Delta FZ}-\sigma_{13}\right)$	$\frac{1}{L_Y}\left(\frac{\Delta(RX1+RX2)}{\Delta FY}-\sigma_{12}\right)$
2	$\frac{\Delta RY1}{\Delta FX}$	$\frac{\Delta RY1}{\Delta FY}$	$\frac{\Delta RY1}{\Delta FZ}$	$\frac{1}{L_R}\left(\frac{\Delta RY1}{\Delta FZ}-\sigma_{23}\right)$	$\frac{1}{L_Y}\left(\frac{\Delta RY1}{\Delta FY}-\sigma_{22}\right)$
3	$\frac{\Delta RY2}{\Delta FX}$	$\frac{\Delta RY2}{\Delta FY}$	$\frac{\Delta RY2}{\Delta FZ}$	$\frac{1}{L_R}\left(\frac{\Delta RY2}{\Delta FZ}-\sigma_{33}\right)$	$\frac{1}{L_Y}\left(\frac{\Delta RY2}{\Delta FY}-\sigma_{32}\right)$
4	$\frac{\Delta(RZ1+RZ3)}{\Delta FX}$	$\frac{\Delta(RZ1+RZ3)}{\Delta FY}$	$\frac{\Delta(RZ1+RZ3)}{\Delta FZ}$	$\frac{1}{L_R}\left(\frac{\Delta(RZ1+RZ3)}{\Delta FZ}-\sigma_{43}\right)$	$\frac{1}{L_Y}\left(\frac{\Delta(RZ1+RZ3)}{\Delta FY}-\sigma_{42}\right)$
5	$\frac{\Delta(RZ2+RZ4)}{\Delta FX}$	$\frac{\Delta(RZ2+RZ4)}{\Delta FY}$	$\frac{\Delta(RZ2+RZ4)}{\Delta FZ}$	$\frac{1}{L_R}\left(\frac{\Delta(RZ2+RZ4)}{\Delta FZ}-\sigma_{53}\right)$	$\frac{1}{L_Y}\left(\frac{\Delta(RZ2+RZ4)}{\Delta FY}-\sigma_{52}\right)$

Table V: Coefficients μ_{ij} for the $[U]^{-1}$ Matrix

$i \diagdown j$	1	2	3	4	5
1	$\frac{\Delta(RX1+RX2)}{\Delta FX}$	$\frac{\Delta(RX1+RX2)}{\Delta FY}$	$\frac{\Delta(RX1+RX2)}{\Delta FZ}$	$\frac{1}{L_P}\left(\frac{\Delta(RX1+RX2)}{\Delta FZ}-\mu_{13}\right)$	$\frac{1}{L_Y}\left(\frac{\Delta(RX1+RX2)}{\Delta FY}-\mu_{12}\right)$
2	$\frac{\Delta RY1}{\Delta FX}$	$\frac{\Delta RY1}{\Delta FY}$	$\frac{\Delta RY1}{\Delta FZ}$	$\frac{1}{L_P}\left(\frac{\Delta RY1}{\Delta FZ}-\mu_{23}\right)$	$\frac{1}{L_Y}\left(\frac{\Delta RY1}{\Delta FY}-\mu_{22}\right)$
3	$\frac{\Delta RY2}{\Delta FX}$	$\frac{\Delta RY2}{\Delta FY}$	$\frac{\Delta RY2}{\Delta FZ}$	$\frac{1}{L_P}\left(\frac{\Delta RY2}{\Delta FZ}-\mu_{33}\right)$	$\frac{1}{L_Y}\left(\frac{\Delta RY2}{\Delta FY}-\mu_{32}\right)$
4	$\frac{\Delta(RZ1+RZ2)}{\Delta FX}$	$\frac{\Delta(RZ1+RZ2)}{\Delta FY}$	$\frac{\Delta(RZ1+RZ2)}{\Delta FZ}$	$\frac{1}{L_P}\left(\frac{\Delta(RZ1+RZ2)}{\Delta FZ}-\mu_{43}\right)$	$\frac{1}{L_Y}\left(\frac{\Delta(RZ1+RZ2)}{\Delta FY}-\mu_{42}\right)$
5	$\frac{\Delta(RZ3+RZ4)}{\Delta FX}$	$\frac{\Delta(RZ3+RZ4)}{\Delta FY}$	$\frac{\Delta(RZ3+RZ4)}{\Delta FZ}$	$\frac{1}{L_P}\left(\frac{\Delta(RZ3+RZ4)}{\Delta FZ}-\mu_{53}\right)$	$\frac{1}{L_Y}\left(\frac{\Delta(RZ3+RZ4)}{\Delta FY}-\mu_{52}\right)$

CONCLUSION

This report documents the derivation of the interaction matrix for the six-component thrust stand in the NASA Glenn Research Center's CE–22 Advanced Nozzle Test Facility. It is intended to give the reader a better understanding of the theory behind the calibration and also insight into how the interaction coefficients are used during testing. Although the equations derived in the paper are specific to the thrust stand in the CE–22 Test Facility, the theory and procedure can be applied to other similar thrust stands.

APPENDIX A—SAMPLE DATA

Tables A1 to A9 show the raw data acquired from a typical calibration. The first column is the applied load, which is measured through the calibration load cells. The other columns are the reaction load cell readings for that particular applied load. All the load cell readings are in units of lbs-force.

In order to reduce the data, each column of reaction load cell readings is plotted against the applied load. The slope of each plot is determined and is shown in bold below each column of reaction load cell readings. The slopes are then plugged into the appropriate equations in Tables IV and V to obtain the $[S]^{-1}$ and $[U]^{-1}$ matrices as shown in equations (A1) and (A2), respectively. Finally, the matrices are inverted to obtain the interaction matrices, $[S]$ and $[U]$, as shown in equations (A3) and (A4), respectively.

NOTE: The slopes can be determined without plotting the data by using the SLOPE function from a spreadsheet application or by using some other curve fitting application. However, it is recommended that the plots be made to verify that the relationships are linear and that the load cell readings are repeatable. A non-linear relationship or non-repeating load cell readings may indicate possible impingement or other problems with the thrust stand.

When plotting the reaction load cell readings that are in-line with the applied load (i.e., $RX1 + RX2$ versus FX), it may be easier to spot any non-linearity by plotting the differences ($RX1 - \frac{FX}{2}$ and $RX2 - \frac{FY}{2}$ versus FX). For the FY calibration data (Table A2), plot $RY1 - \frac{FY}{2}$ and $RY2 - \frac{FY}{2}$ versus FY, etc.

Table A1.—Reaction Load Cell Data for an Applied Axial (*FX*) Calibration Load

	FX	RX1+RX2	RY1	RY2	RZ1+RZ3	RZ2+RZ4	RZ1+RZ2	RZ3+RZ4
	-0.076	0.08116	-0.01616	0.09777	0.00806	-0.02446	-0.01633	-0.00007
	-248.273	-244.18423	-0.01621	0.18475	-2.11985	1.62589	0.13440	-0.62837
	-496.850	-488.36049	0.00556	0.55398	-3.68300	1.41625	-0.11567	-2.15108
	-741.769	-728.80176	-0.13496	1.31452	-5.17018	0.96820	-0.43034	-3.77164
	-995.160	-977.71618	-0.12427	1.94453	-6.74403	0.67170	-0.76709	-5.30524
	-1191.340	-1170.86760	-0.05919	2.24859	-7.97051	0.46239	-0.87602	-6.63210
	-1506.270	-1479.90848	-0.12404	3.03074	-9.80519	-0.05211	-1.28864	-8.56866
	-1749.960	-1718.99245	-0.19981	3.57396	-11.28090	-0.39213	-1.59284	-10.08020
	-1996.210	-1960.87038	-0.17816	4.31263	-12.74650	-0.56914	-1.76691	-11.54870
	-2247.730	-2208.06632	-0.22164	4.85580	-14.57040	-0.90945	-2.16884	-13.31100
	-2493.760	-2449.83597	-0.23233	5.37711	-16.13370	-0.95618	-2.31041	-14.77950
	-2245.690	-2206.30791	-0.18907	4.39948	-14.41840	-0.92054	-2.04962	-13.28930
	-1988.620	-1953.47239	-0.12416	4.11726	-12.90930	-0.54764	-1.76706	-11.68990
	-1716.560	-1686.63940	-0.13479	3.61741	-11.46590	-0.20700	-1.56037	-10.11260
	-1502.470	-1475.90281	-0.14576	3.00909	-9.77222	-0.11735	-1.38639	-8.50318
	-1227.920	-1206.20993	-0.10233	2.55280	-8.07914	0.25593	-0.97344	-6.84978
	-1082.120	-1062.68568	-0.12427	1.90087	-6.97162	0.31164	-0.79985	-5.86013
	-734.171	-721.45830	-0.05919	1.20591	-5.07227	0.95752	-0.43040	-3.68436
	-504.028	-495.20946	-0.02696	0.64099	-3.49827	1.23252	-0.14781	-2.11794
	-256.595	-252.18475	-0.10273	0.07607	-2.10914	1.56145	0.08039	-0.62808
	-2.034	-2.52099	0.08132	0.07605	0.09475	-0.08899	0.11404	-0.10827
Slope		**9.82289E-01**	**9.03304E-05**	**-2.21641E-03**	**6.33701E-03**	**8.45466E-04**	**1.03865E-03**	**6.14383E-03**

Table A2.—Reaction Load Cell Data for an Applied Lateral (*FY*) Calibration Load

	FY	RX1+RX2	RY1	RY2	RZ1+RZ3	RZ2+RZ4	RZ1+RZ2	RZ3+RZ4
	0.173	1.72279	0.13895	-0.03260	0.16653	-0.56756	0.46330	-0.86432
	-199.017	1.02173	-100.04375	-98.23386	3.97433	-1.77150	0.88328	1.31955
	-398.089	0.23809	-200.01456	-196.67408	7.87209	-3.33785	1.58827	2.94597
	-598.639	-0.56701	-300.66609	-295.65779	11.78050	-4.82801	2.38028	4.57224
	-798.102	-0.91570	-400.87485	-393.57694	15.70010	-6.34095	3.19351	6.16569
	-997.770	-1.67719	-501.96905	-490.97454	19.54380	-7.89665	3.84427	7.80289
	-802.978	-1.02454	-404.80565	-394.16332	15.82020	-6.30867	3.28020	6.23133
	-599.496	-0.04541	-301.61662	-294.59337	11.85740	-4.69863	2.55357	4.60522
	-400.315	0.08629	-201.55894	-196.28306	7.91596	-3.26284	1.83762	2.81550
	-201.223	0.80389	-101.04839	-98.56003	4.04029	-1.87035	0.93740	1.23254
	-1.554	0.03669	-0.23489	-0.05432	0.01238	-0.10756	0.05897	-0.15415
	-1.586	-0.11380	-0.33209	-0.16295	-0.05281	-0.08541	-0.11456	-0.02366
	101.302	1.52951	50.76034	50.52374	-1.93118	0.60003	-0.36404	-0.96711
	201.191	1.59489	100.92412	99.79834	-3.97234	1.10063	-0.81932	-2.05239
	400.904	2.68374	201.01400	198.15191	-8.13028	2.61184	-1.67641	-3.84204
	600.083	3.38000	300.98468	296.46167	-12.29910	3.97063	-2.55511	-5.77337
	800.849	4.37951	401.78705	394.98880	-16.51100	5.18873	-3.75893	-7.56330
	1000.140	5.53105	500.99188	494.05984	-20.78820	6.56933	-4.81114	-9.40776
	802.121	4.16295	402.15437	395.94487	-16.51130	5.37297	-3.68327	-7.45502
	601.170	3.05559	301.20069	297.22208	-12.37520	3.99214	-2.73962	-5.64340
	401.739	2.42511	201.78045	198.45576	-8.19559	2.57888	-1.85003	-3.76667
	201.462	1.87866	101.19412	99.75490	-4.03738	1.29532	-0.88477	-1.85730
	-0.978	-0.15674	-0.27809	0.29330	0.02375	0.06488	-0.01737	0.10600
Slope		**3.24399E-03**	**5.02184E-01**	**4.93022E-01**	**-2.01384E-02**	**7.27373E-03**	**-4.32204E-03**	**-8.54266E-03**

Table A3.—Reaction Load Cell Data for an Applied Vertical (*FZ*) Calibration Load

	FZ	RX1+RX2	RY1	RY2	RZ1+RZ3	RZ2+RZ4	RZ1+RZ2	RZ3+RZ4
	-0.182	0.21096	0.30270	0.60352	0.13023	-0.18184	0.03653	-0.08813988
	-122.114	-0.05653	-0.07552	0.32083	-66.93741	-55.36818	-54.47783	-67.82777
	-195.405	0.23145	-0.56161	1.34201	-97.10230	-98.53182	-96.38174	-99.25238
	-396.876	0.22783	-1.57722	2.23274	-198.22435	-198.27911	-196.30354	-200.1999
	-595.704	0.50627	-2.75482	3.16696	-296.37602	-299.01475	-295.29661	-300.09413
	-797.505	1.12958	-4.26704	4.05733	-397.00668	-400.08529	-394.08145	-403.01053
	-997.280	1.23316	-5.89845	4.86111	-496.76134	-500.42699	-492.58238	-504.60594
	-791.401	0.95530	-4.53703	3.97054	-398.04806	-393.37946	-396.69803	-394.729492
	-591.878	0.67832	-2.99241	3.03643	-298.45871	-293.26227	-297.69742	-294.02356
	-394.760	0.05386	-1.98743	2.12405	-198.56521	-196.20239	-198.00744	-196.760157
	-195.468	-0.15899	-0.82068	1.42891	-99.61442	-95.92333	-98.43285	-97.104903
	-0.356	-0.20055	0.11916	0.75566	-0.17747	-0.29079	-0.10239	-0.365874
	-0.356	-0.19993	0.32447	0.90763	-0.17726	-0.13897	-0.09167	-0.2245624
	106.225	-0.24085	0.69159	0.21243	46.97258	57.96355	49.80986	55.12627
	202.897	-0.19520	1.19928	-0.15672	99.61429	101.53351	99.13997	102.007826
	403.314	-0.47372	2.33398	-0.78666	199.54785	201.64844	197.65555	203.54074
	600.397	-0.66589	3.18777	-1.63400	297.89018	300.25246	294.77751	303.3651
	802.781	-0.85736	3.92213	-2.22038	398.75876	401.35678	395.11877	404.99676
	1003.720	-1.20230	4.46257	-3.08939	499.73613	501.06468	495.28984	505.51097
	799.046	-0.88040	4.00847	-2.22038	398.36290	397.90517	395.61348	400.65459
	601.312	-0.96911	3.28428	-1.67740	299.70144	299.31722	298.16332	300.855371
	403.950	-0.30180	2.43060	-0.96061	200.67799	200.96201	200.02221	201.617792
	203.367	-0.02257	1.59869	-0.02642	99.55675	101.63349	101.00390	100.18635
	-0.215	0.25533	0.52920	0.71212	-0.61246	-0.06636	-0.52553	-0.1533004
Slope		**-1.12824E-03**	**5.18577E-03**	**-3.91494E-03**	**4.98625E-01**	**4.99398E-01**	**4.95026E-01**	**5.02996E-01**

Table A4.—Reaction Load Cell Data for an Applied Rolling (*MX*) Calibration Moment (*CZ*2+*CZ*4)

FZ(CZ2+CZ4)	RX1+RX2	RY1	RY2	RZ1+RZ3	RZ2+RZ4
-0.095	0.40605	-0.01889	0.09239	0.07597	0.02983
-98.092	0.94584	-0.84028	0.33126	-0.05302	-97.98530
-198.716	1.39963	-1.68273	0.87454	-0.39818	-198.12115
-285.066	1.83268	-2.63401	1.20041	-0.55856	-284.14577
-395.603	3.25951	-3.37940	1.83042	-0.60134	-394.51621
-496.671	4.27402	-4.41651	2.19956	-0.69548	-496.05751
-393.718	3.17302	-3.45507	1.69988	-0.42769	-393.19346
-295.635	1.96152	-2.75224	1.30906	-0.22750	-295.24944
-203.242	1.42101	-1.88824	0.98313	-0.07828	-203.02438
-98.304	0.55617	-0.86167	0.37476	-0.02587	-98.40839
0.122	0.27647	-0.09461	0.11414	0.24322	-0.10298
0.122	0.57843	-0.24616	-0.01630	0.22144	-0.15732
47.468	0.18941	0.53234	-0.19004	0.41537	46.29615
101.030	-0.54614	1.09372	-0.47258	0.58859	99.58819
201.307	-1.13021	2.28243	-1.03742	0.84653	199.45385
301.505	-1.67007	3.25461	-1.40687	1.06070	299.19772
393.713	-2.01518	4.15151	-1.64560	1.25342	391.15047
502.798	-2.68565	5.19957	-2.10197	1.51171	499.99444
400.466	-2.34019	4.11889	-1.66738	1.21956	397.95660
314.838	-2.12538	3.30868	-1.47203	1.02598	312.82024
203.245	-1.15181	2.24997	-1.01581	0.76717	201.71789
102.645	-0.54578	1.13709	-0.53788	0.42314	101.65790
0.068	0.31917	0.02432	0.44014	-0.04047	0.99723
Slope	**-6.70280E-03**	**9.71169E-03**	**-4.40648E-03**	**2.29953E-03**	**9.95765E-01**

Table A5.—Reaction Load Cell Data for an Applied Rolling (*MX*) Calibration Moment (*CZ*1+*CZ*3)

FZ(CZ1+CZ3)	RX1+RX2	RY1	RY2	RZ1+RZ3	RZ2+RZ4
-0.119	0.00983	0.04071	0.13592	-0.02980	-0.02729
-96.137	-0.53339	-0.11055	0.26619	-95.73914	-0.36048
-196.837	-0.92484	-0.24037	0.76593	-196.04780	-0.72147
-296.575	-1.62091	-0.47803	1.02671	-295.17781	-1.10289
-398.164	-2.29420	-0.96460	1.50476	-396.79452	-1.18055
-496.597	-2.75075	-1.32089	1.80889	-495.14043	-1.42026
-400.760	-2.44669	-1.14792	1.63503	-399.37456	-1.21455
-300.914	-1.77205	-0.81278	1.17878	-299.74948	-0.86274
-201.142	-1.03284	-0.55352	0.72244	-200.40714	-0.48717
-102.089	-0.38129	-0.51004	0.41839	-101.68782	-0.18457
0.097	-0.16213	-0.34821	0.09239	0.15703	0.08560
0.075	0.20449	-0.33752	0.11405	0.17888	0.09594
100.807	0.40289	-0.49924	-0.29874	99.76244	0.31821
200.548	0.59911	-0.45592	-0.66822	199.07447	0.66960
301.766	1.25080	-0.60673	-0.71150	299.99751	0.93793
399.612	1.40378	-0.83325	-1.16765	397.36804	1.28183
501.018	1.79513	-1.11411	-1.75457	498.13647	1.63925
402.179	1.79429	-0.72559	-1.38518	399.86265	1.12246
302.363	1.27253	-0.46667	-1.05934	300.71554	0.86332
203.724	0.98929	-0.18570	-0.58125	202.27007	0.61982
104.093	0.31563	-0.18620	-0.21176	102.98550	0.27447
-0.185	0.00966	-0.05688	0.04890	-0.03888	-0.15213
Slope	**4.76143E-03**	**2.44622E-04**	**-3.48135E-03**	**9.95250E-01**	**3.05296E-03**

Table A6.—Reaction Load Cell Data for an Applied Pitching (*MY*) Calibration Moment (*CZ*3+*CZ*4)

FZ(CZ3+CZ4)	RX1+RX2	RY1	RY2	RZ1+RZ2	RZ3+RZ4
0.114	0.08619	-0.02446	-0.06535	-0.17562	-0.02855
-95.967	0.17060	-0.01371	0.47773	-0.05575	-95.91599
-197.705	0.51364	-0.02435	0.89045	-0.03389	-197.54135
-294.995	0.96501	-0.04612	1.52049	0.05348	-294.69016
-398.320	1.02797	-0.06789	2.06354	-0.09816	-398.02602
-493.010	1.19765	-0.04634	2.71528	-0.13032	-493.12850
-420.868	1.39415	-0.02468	2.21573	-0.13051	-420.70852
-305.238	0.98726	-0.04606	1.65078	-0.19556	-305.13699
-202.474	0.59973	-0.02462	1.06422	-0.01232	-202.40378
-105.353	0.19133	0.02972	0.56467	-0.08825	-105.27046
-0.136	-0.00148	0.02983	-0.08707	0.04166	0.02727
-0.104	-0.08750	0.02978	-0.02192	-0.13168	-0.01627
98.888	-0.36710	-0.02440	-0.65203	0.01987	98.10948
202.037	-0.60105	-0.08927	-1.30360	0.03052	201.26211
298.033	-0.75012	0.01925	-1.97712	-0.02396	297.18196
388.805	-0.94450	0.06268	-2.45499	0.03009	388.02860
503.682	-1.22189	-0.02390	-3.04142	0.16009	502.71252
414.068	-0.85563	-0.01332	-2.36803	0.17226	413.16904
324.285	-0.62045	-0.03493	-1.84660	-0.03363	323.33389
211.681	-0.53763	-0.05648	-1.12968	-0.07730	210.67912
102.710	-0.12880	-0.05675	-0.36938	-0.04404	101.80023
0.071	0.15041	-0.11098	-0.10883	-0.02210	0.20512
Slope	**-2.58132E-03**	**3.43725E-05**	**-5.64588E-03**	**2.07362E-04**	**9.98524E-01**

Table A7.—Reaction Load Cell Data for an Applied Pitching (*MY*) Calibration Moment (*CZ*1+*CZ*2)

FZ(CZ1+CZ2)	RX1+RX2	RY1	RY2	RZ1+RZ2	RZ3+RZ4
-0.057	-0.08672	0.07834	0.13033	-0.05664	-0.02931
-98.239	0.06304	-0.90529	0.19539	-97.89613	-0.05817
-198.364	0.04114	-2.03966	0.34740	-197.72341	-0.23136
-297.111	-0.32899	-3.14136	0.69507	-296.45896	-0.22986
-394.386	-0.17731	-4.58892	1.17299	-393.53480	-0.41979
-495.419	0.05887	-6.13363	1.39012	-494.32711	-0.58019
-401.170	-0.41605	-4.89115	0.99907	-400.04213	-0.46138
-301.643	0.01994	-3.35696	1.04276	-300.91763	-0.33220
-200.902	-0.32668	-2.34172	0.47775	-200.28124	-0.24733
-100.386	-0.21731	-1.26117	0.26045	-99.94337	-0.27722
0.203	0.12980	-0.36496	0.15200	0.30889	-0.04212
-0.057	0.15178	-0.21325	0.15208	0.29809	0.02324
99.436	0.17428	0.67216	-0.19566	98.69910	0.06921
199.062	-0.17067	1.68802	-0.47797	198.07608	0.25585
299.204	0.15444	2.62766	-0.54303	298.00783	0.23338
396.699	0.11222	3.36261	-0.89077	395.36138	0.37850
498.648	0.02432	4.03259	-0.91242	497.10607	0.33736
426.118	-0.27832	3.65409	-0.82546	424.58068	0.39550
307.580	-0.14877	2.91953	-0.73865	306.55375	0.34494
204.004	-0.01904	2.08739	-0.36915	203.02115	0.18254
103.048	0.28332	1.06090	-0.17367	102.25487	0.10756
-0.491	0.19501	0.01309	0.08694	-0.30891	-0.04760
Slope	**1.87379E-04**	**1.01435E-02**	**-2.36003E-03**	**9.96940E-01**	**9.95332E-04**

Table A8.— Reaction Load Cell Data for an Applied Yawing (*MZ*) Calibration Moment (*CY*1)

FY(CY1)	RX1+RX2	RY1	RY2	RZ1+RZ3	RZ2+RZ4	RZ1+RZ2	RZ3+RZ4
-0.060	0.34636	0.00540	0.09244	-0.14667	0.07093	-0.09759	0.02185
-98.736	-0.47761	-99.35273	1.11350	2.55698	-1.73772	0.78066	0.03859
-196.999	-0.06588	-198.65658	1.89511	5.11851	-3.71743	1.37741	0.02367
-296.414	-0.19644	-298.79272	3.17686	7.70208	-5.64329	1.99568	0.06311
-397.479	0.14908	-400.80795	4.30644	10.55750	-7.53678	2.73333	0.28740
-497.490	-0.17515	-501.86122	5.39250	12.92390	-9.66888	3.08069	0.17431
-401.864	0.08408	-405.39702	4.19760	10.59010	-7.71076	2.69005	0.18931
-301.310	0.23670	-303.82511	3.17683	7.85460	-5.64357	2.00658	0.20445
-202.330	-0.08751	-203.89467	1.98213	5.08622	-3.67457	1.43141	-0.01976
-102.221	-0.04392	-102.71136	1.00481	2.46999	-1.83554	0.72635	-0.09190
-0.733	0.23846	-0.22140	-0.01628	-0.19006	0.02653	-0.07603	-0.08751
-0.842	-0.19514	-0.25380	0.11423	-0.01623	0.01571	0.01077	-0.01129
99.735	0.13095	99.98992	-1.03731	-2.79619	2.18243	-0.41219	-0.20157
197.792	0.54200	198.72198	-1.73204	-5.62926	4.16256	-1.26918	-0.19752
297.868	0.65163	299.10552	-2.62260	-8.26698	5.88162	-2.05029	-0.33507
397.706	0.89018	399.20908	-3.38277	-10.93720	7.77434	-2.75537	-0.40747
497.544	1.19370	499.29104	-4.22984	-13.80250	9.59137	-3.70989	-0.50122
402.266	1.30217	403.76673	-3.33931	-11.07860	7.93806	-2.76624	-0.37431
303.601	0.67313	304.70024	-2.79655	-8.36532	5.92616	-2.03915	-0.40002
202.754	0.32711	203.35530	-1.99296	-5.53228	4.13155	-1.31232	-0.08841
102.644	0.30529	103.07865	-0.90669	-2.77503	2.07552	-0.56359	-0.13593
-0.299	0.15410	-0.29699	0.04896	0.01499	-0.03513	0.05490	-0.07504
Slope	**1.26865E-03**	**1.00607E+00**	**-9.63870E-03**	**-2.68759E-02**	**1.93614E-02**	**-6.79093E-03**	**-7.23528E-04**

Table A9.—Reaction Load Cell Data for an Applied Yawing (*MZ*) Calibration Moment (*CY*2)

FY(CY2)	RX1+RX2	RY1	RY2	RZ1+RZ3	RZ2+RZ4	RZ1+RZ2	RZ3+RZ4
0.122	-0.27797	-0.00013	0.00000	-0.19291	-0.01109	-0.14659	-0.05741
-98.354	1.05326	-0.02201	-97.73551	1.31651	0.00043	0.03793	1.27901
-195.700	-0.09698	-0.13074	-194.94930	2.47839	0.50088	0.18960	2.78967
-297.907	-0.35991	-0.12028	-297.05226	3.80308	0.90376	0.40640	4.30044
-392.284	-0.99036	-0.19633	-390.57267	5.11724	1.45849	0.60145	5.97428
-486.835	-1.72973	-0.14288	-484.96217	6.36609	1.81731	0.79642	7.38697
-404.638	-1.09835	-0.16381	-402.97931	5.13934	1.50159	0.55786	6.08307
-306.325	-0.51151	-0.17439	-305.00536	3.96669	1.09907	0.48232	4.58344
-210.687	0.07625	-0.22795	-209.72551	2.76120	0.52253	0.26554	3.01819
-105.826	0.94605	-0.16236	-105.31903	1.51264	0.08697	0.17889	1.42072
-0.084	-0.10406	-0.09727	-0.13037	-0.16004	-0.13053	-0.11388	-0.17669
-0.095	-0.19144	-0.04288	-0.08692	-0.15998	-0.04380	-0.08137	-0.12241
97.849	1.75407	-0.12940	97.62693	-1.48436	-0.92545	-0.34154	-2.06827
195.956	2.25764	0.00116	195.53638	-2.85236	-1.35007	-0.59093	-3.61149
294.585	2.45579	-0.03074	293.66294	-4.11190	-1.77491	-0.68830	-5.19851
394.236	2.99926	0.05651	392.96253	-5.63228	-2.21091	-0.82937	-7.01382
493.790	3.71653	0.12176	492.08922	-7.00022	-2.65797	-0.91597	-8.74222
411.604	3.45377	0.14275	410.28030	-5.92587	-2.36298	-0.93769	-7.35116
327.352	3.03964	0.10939	326.14689	-4.55752	-1.92726	-0.76420	-5.72058
201.709	1.82409	0.13060	201.27272	-2.96133	-1.16533	-0.49331	-3.63335
105.679	1.69122	0.00010	105.31893	-1.54982	-0.76203	-0.41737	-1.89448
-0.019	0.32908	-0.03247	0.06518	-0.13802	0.02135	-0.13558	0.01890
Slope	**5.30436E-03**	**3.39443E-04**	**9.96382E-01**	**-1.36043E-02**	**-4.61535E-03**	**-1.84459E-03**	**-1.63751E-02**

The Inverse Matrices

$$[S]^{-1} = \begin{bmatrix} 9.82289E\text{-}01 & 3.24399E\text{-}03 & -1.12824E\text{-}03 & -5.21101E\text{-}04 & -1.13682E\text{-}04 \\ 9.03304E\text{-}05 & 5.02184E\text{-}01 & 5.18577E\text{-}03 & 4.30321E\text{-}04 & 2.83304E\text{-}02 \\ -2.21641E\text{-}03 & 4.93022E\text{-}01 & -3.91494E\text{-}03 & -4.20514E\text{-}05 & -2.83386E\text{-}02 \\ 6.33701E\text{-}03 & -2.01384E\text{-}02 & 4.98625E\text{-}01 & -4.51341E\text{-}02 & -3.73846E\text{-}04 \\ 8.45466E\text{-}04 & 7.27373E\text{-}03 & 4.99398E\text{-}01 & 4.51233E\text{-}02 & 6.75402E\text{-}04 \end{bmatrix} \tag{A1}$$

$$[U]^{-1} = \begin{bmatrix} 9.82289E\text{-}01 & 3.24399E\text{-}03 & -1.12824E\text{-}03 & -6.25890E\text{-}05 & -1.13682E\text{-}04 \\ 9.03304E\text{-}05 & 5.02184E\text{-}01 & 5.18577E\text{-}03 & -2.28486E\text{-}04 & 2.83304E\text{-}02 \\ -2.21641E\text{-}03 & 4.93022E\text{-}01 & -3.91494E\text{-}03 & -7.42812E\text{-}05 & -2.83386E\text{-}02 \\ 1.03865E\text{-}03 & -4.32204E\text{-}03 & 4.95026E\text{-}01 & -2.25248E\text{-}02 & -1.39334E\text{-}04 \\ 6.14383E\text{-}03 & -8.54266E\text{-}03 & 5.02996E\text{-}01 & 2.25429E\text{-}02 & 4.40889E\text{-}04 \end{bmatrix} \tag{A2}$$

The Interaction Matrices

$$[S] = \begin{bmatrix} 1.01804 & -1.55676E\text{-}03 & -5.41036E\text{-}03 & -4.74953E\text{-}03 & 7.01590E\text{-}03 \\ 2.15971E\text{-}03 & 1.00515 & 1.00467 & 3.03588E\text{-}03 & -5.58783E\text{-}03 \\ -7.28563E\text{-}03 & 7.67051E\text{-}03 & 1.83743E\text{-}02 & 1.00195 & 1.00206 \\ 6.18255E\text{-}02 & -5.08750E\text{-}01 & -9.85532E\text{-}02 & -11.0884 & 11.0759 \\ -4.11345E\text{-}02 & 17.4869 & -17.8107 & -6.87765E\text{-}02 & -2.52631E\text{-}01 \end{bmatrix} \tag{A3}$$

$$[U] = \begin{bmatrix} 1.01800 & -1.29503E\text{-}03 & -5.33780E\text{-}03 & -2.72514E\text{-}04 & 2.52342E\text{-}03 \\ 2.14928E\text{-}03 & 1.00491 & 1.00473 & -8.08604E\text{-}03 & 5.42246E\text{-}03 \\ -7.28416E\text{-}03 & 7.67704E\text{-}03 & 1.83836E\text{-}02 & 1.00235 & 1.00166 \\ -1.13301E\text{-}01 & -1.32250E\text{-}01 & 3.21076E\text{-}01 & -22.3640 & 22.0132 \\ -4.09244E\text{-}02 & 17.4823 & -17.8106 & -2.20509E\text{-}01 & -1.01940E\text{-}01 \end{bmatrix} \tag{A4}$$

REFERENCES

1. Luis Beltran, Richard L. Del Roso, and Ruben Del Rosario, "Advanced Nozzle and Engine Components Test Facility," NASA Technical Memorandum 103684, January 1992.
2. Joyel M. Kerl, Gwynn A. Severt, and Kurt Loos, "Advanced Nozzle Test Facility at NASA Glenn Research Center," AIAA–2002–3245, June 2002.

REPORT DOCUMENTATION PAGE

Form Approved
OMB No. 0704-0188

Public reporting burden for this collection of information is estimated to average 1 hour per response, including the time for reviewing instructions, searching existing data sources, gathering and maintaining the data needed, and completing and reviewing the collection of information. Send comments regarding this burden estimate or any other aspect of this collection of information, including suggestions for reducing this burden, to Washington Headquarters Services, Directorate for Information Operations and Reports, 1215 Jefferson Davis Highway, Suite 1204, Arlington, VA 22202-4302, and to the Office of Management and Budget, Paperwork Reduction Project (0704-0188), Washington, DC 20503.

1. AGENCY USE ONLY (*Leave blank*)

2. REPORT DATE
April 2003

3. REPORT TYPE AND DATES COVERED
Technical Memorandum

4. TITLE AND SUBTITLE
Derivation of the Data Reduction Equations for the Calibration of the Six-Component Thrust Stand in the CE–22 Advanced Nozzle Test Facility

5. FUNDING NUMBERS
WBS–22–708–90–66

6. AUTHOR(S)
Kin C. Wong

7. PERFORMING ORGANIZATION NAME(S) AND ADDRESS(ES)
National Aeronautics and Space Administration
John H. Glenn Research Center at Lewis Field
Cleveland, Ohio 44135–3191

8. PERFORMING ORGANIZATION REPORT NUMBER
E–13921

9. SPONSORING/MONITORING AGENCY NAME(S) AND ADDRESS(ES)
National Aeronautics and Space Administration
Washington, DC 20546–0001

10. SPONSORING/MONITORING AGENCY REPORT NUMBER
NASA TM—2003-212326

11. SUPPLEMENTARY NOTES
Responsible person, Kin C. Wong, organization code 7180, 216–433–8712.

12a. DISTRIBUTION/AVAILABILITY STATEMENT
Unclassified - Unlimited
Subject Category: 09 Distribution: Nonstandard
Available electronically at http://gltrs.grc.nasa.gov
This publication is available from the NASA Center for AeroSpace Information, 301–621–0390.

12b. DISTRIBUTION CODE

13. ABSTRACT ***(Maximum 200 words)***

This paper documents the derivation of the data reduction equations for the calibration of the six-component thrust stand located in the CE–22 Advanced Nozzle Test Facility. The purpose of the calibration is to determine the first-order interactions between the axial, lateral, and vertical load cells (second-order interactions are assumed to be negligible). In an ideal system, the measurements made by the thrust stand along the three coordinate axes should be independent. For example, when a test article applies an axial force on the thrust stand, the axial load cells should measure the full magnitude of the force, while the off-axis load cells (lateral and vertical) should read zero. Likewise, if a lateral force is applied, the lateral load cells should measure the entire force, while the axial and vertical load cells should read zero. However, in real-world systems, there may be interactions between the load cells. Through proper design of the thrust stand, these interactions can be minimized, but are hard to eliminate entirely. Therefore, the purpose of the thrust stand calibration is to account for these interactions, so that necessary corrections can be made during testing. These corrections can be expressed in the form of an interaction matrix, and this paper shows the derivation of the equations used to obtain the coefficients in this matrix.

14. SUBJECT TERMS
Thrust measurement; Loads (forces); Nozzle thrust coefficients; Thrust loads; Test stands; Test facilities; Transducers; Pitching moments; Yawing moments; Rolling moments; Thrust vector control

15. NUMBER OF PAGES
36

16. PRICE CODE

17. SECURITY CLASSIFICATION OF REPORT	18. SECURITY CLASSIFICATION OF THIS PAGE	19. SECURITY CLASSIFICATION OF ABSTRACT	20. LIMITATION OF ABSTRACT
Unclassified	Unclassified	Unclassified	